JOURNAL OF GREEN COMPLEX ENGINEERING, 2026, Vol.4, No.1, 89~98
https://doi.org/10.59810/greenplexresearch.v4i1.292
e-ISSN 3025-9673

Asymmetric Bank Erosion Reveals Geomorphic Susceptibility in the Pattalasang River, Indonesia

Sri Winanda*, Marufah, Muh Yunus Ali

Department of Water Resources Engineering, Faculty of Engineering, Universitas Muhammadiyah Makassar, Makassar, Indonesia

ABSTRACT

Riverbank erosion can alter channel geometry and progressively reduce bank support, yet reconnaissance studies often lack the hydraulic and geotechnical data required for formal stability modelling. This study evaluates whether simple field measurements can provide a defensible screening of geomorphic susceptibility along the Pattalasang River, South Sulawesi, Indonesia. Three cross-sections were examined: one comparatively stable baseline and two eroding sites. Cross-sectional areas were reconstructed by trapezoidal integration, erosion volumes were calculated from measured erosion dimensions, lateral concentration was expressed using an asymmetry index, and two grain-size distributions were compared descriptively. Quality control corrected a factor-of-four inconsistency in the original cross-sectional summaries, giving areas of 17.55, 14.70, and 13.25 m² for the baseline, Point I, and Point II. Erosion volume reached 74.96 m³ at Point I and 25.41 m³ at Point II. Left-bank erosion contributed 92.45% and 89.10% of site totals, with asymmetry indices of 0.849 and 0.782. Similar grain-size curves indicate that sediment gradation alone does not explain the 2.95-fold erosion contrast. The screening identifies Point I as the priority for repeat hydraulic and geotechnical assessment.

ARTICLE HISTORY

Received June 25, 2026
Received in revised form July 25, 2026
Accepted August 20, 2026
Available online August 28, 2026.

KEYWORDS

riverbank erosion; geomorphic susceptibility; channel cross-section; bank retreat; tropical river

1. Introduction

Riverbank erosion is a boundary-adjustment process through which flowing water, sediment transport, bank material, vegetation, and channel geometry jointly reshape the river corridor. At the reach scale, erosion can narrow or widen individual cross-sections, shift banklines, reorganize bars and thalwegs, and expose riparian land and infrastructure to progressive loss. At larger scales, multitemporal studies consistently show that bank erosion and channel migration are spatially heterogeneous rather than uniformly distributed. Recent work has documented pronounced reach-to-reach contrasts in bank retreat and channel morphology using satellite imagery, historical cross-sections, field surveys, and hydrodynamic observations [1-3]. This heterogeneity is central to river management because a reach that appears stable at one location may coexist with an adjacent erosion hotspot controlled by different local boundary conditions.

Hydraulic attack is a principal driver of this spatial variability. Flow concentration at bends, local acceleration, turbulence, elevated near-bank shear stress, and flood-stage fluctuations can promote bed and toe scour and increase the probability of bank retreat. Field and model evidence from different river settings indicates that near-bank hydraulics can control the location and magnitude of erosion even where broader reach-scale discharge remains similar [2,4,5]. Flood-related planform changes can also be strongly localized, with erosion preferentially affecting particular banks or concave margins [6-8]. Recent open-channel experiments in Makassar further show that increasing discharge intensifies local scour under unprotected conditions and that porous flow-control devices can reduce near-bed velocity, vortex activity, and scour depth [9,10]. Although bridge-pier scour is not equivalent to riverbank erosion, these experiments provide regionally relevant evidence that local flow energy and turbulence govern sediment removal in open-channel settings.

Bank response, however, cannot be reduced to hydraulic forcing alone. Material composition, soil structure, density, cohesion, pore-water conditions, vegetation, and geometric configuration control the resistance available to oppose erosion and mass failure. Recent integrated studies show that bank stability and retreat reflect interactions among channel geometry, soil properties, hydrologic conditions, and geotechnical resistance [11-14]. Grain size is therefore informative but incomplete as a descriptor of erodibility. Experimental and field studies demonstrate that coarse-fraction characteristics, root reinforcement, and soil-biogeochemical properties can alter erosion resistance even when bulk textural classes appear similar [15-18].

The difficulty is that the most mechanistically complete approaches are also the most data-demanding. Process-based tools such as the Bank Stability and Toe Erosion Model and coupled hydro-morphodynamic or geotechnical models require information on hydraulic forcing, erodibility, bank geometry, soil strength, and in some cases groundwater conditions. Comparative modelling shows that model choice matters because simplified form-based indices can miss geotechnical failure or event-scale morphodynamic adjustments that process-based models represent more explicitly [19]. Integrated hydraulic and geotechnical investigations likewise depend on field and laboratory inputs that are rarely available during initial

CONTACT: Sri Winanda xtkjsriwinanda@gmail.com Department of Water Resources Engineering, Faculty of Engineering, Universitas Muhammadiyah Makassar, Makassar, Indonesia

reconnaissance [11,13]. These methods are indispensable for design-level stability analysis but are not always feasible during early screening or resource-limited monitoring.

A parallel body of work therefore emphasizes rapid geomorphic assessment, repeated cross-section monitoring, photogrammetry, and other field-observable indicators. Recent rapid-assessment work shows that continuous geomorphic observation can reveal instability that sparse site metrics may overlook [20], while Structure-from-Motion photogrammetry and repeated topographic surveys provide more detailed volumetric information where resources permit [21]. Reviews of fluvial geomorphology in data-limited regions also note that field-based process studies remain less common than remote-sensing assessments, creating a practical gap between broad mapping and detailed process modelling [22].

This gap is especially important for tropical and rapidly changing river corridors where decisions about monitoring or bank protection must often be made before a complete geotechnical investigation is available. Recent susceptibility and hotspot studies increasingly integrate multiple geomorphic indicators to prioritize unstable reaches [23], and integrated analyses of bank dynamics combine morphology, hydrology, and geotechnical information to improve management relevance [1]. In Sulawesi, Takwim et al. (2025) showed that erosion hazard can vary markedly with land cover and slope and used that spatial variation to define conservation priorities. Yet a smaller, explicitly transparent question remains at the channel scale: how much defensible information can be extracted from a modest field dataset consisting only of cross-sectional geometry, direct erosion dimensions, and basic particle-size data, without converting those observations into an unjustified factor-of-safety claim?

The methodological gap is therefore a mismatch of scale rather than an absence of sophisticated models. Broad mapping identifies where erosion may be important, whereas process-based modelling explains failure only where demanding hydraulic and geotechnical inputs are available. A defensible reconnaissance method should occupy the space between those approaches: it should extract physically interpretable evidence from inexpensive field measurements, identify uncertainty explicitly, and generate hypotheses that can be tested by the next level of monitoring.

The Pattalasang River in Gowa Regency, South Sulawesi, Indonesia, provides an appropriate case for addressing this question. The available field dataset contains three channel cross-sections, direct measurements of visibly eroded bank zones at two points, and grain-size distributions from two bank-material samples. It does not contain concurrent velocity or discharge measurements, cohesion, friction angle, unit weight, pore-water pressure, groundwater records, or repeated temporal surveys. The dataset is therefore insufficient for formal geotechnical stability modelling but suitable for developing a first-tier geomorphic screening approach. The original field-data summary contained a numerical inconsistency in the reported cross-sectional areas, making arithmetic quality control an integral part of the analysis.

Accordingly, this study integrates cross-sectional reconstruction, measured erosion volume, bank-to-bank asymmetry, and grain-size comparison into a field-based diagnostic of physical bank susceptibility. The central hypothesis is that the site with greater measured erosion will also exhibit stronger evidence of localized geometric deterioration, while the contrast between eroding sites will not be explainable by grain-size distribution alone. The objectives are to (1) quantify and compare cross-sectional geometry at a relatively stable baseline and two eroding points; (2) quantify the magnitude and lateral concentration of measured bank erosion; (3) compare the grain-size distributions of bank materials; and (4) interpret these observations within the broader literature on hydraulic attack, bank material resistance, vegetation, monitoring, and geotechnical stability. The intended contribution is a reproducible screening logic that preserves the distinction between geomorphic susceptibility and engineering stability while identifying where more detailed hydraulic and geotechnical investigation should be prioritized.

2. Methods

2.1 Study design and field measurements

The study used a quantitative descriptive field design based on measurements collected along a segment of the Pattalasang River in Gowa Regency, South Sulawesi, Indonesia. Three cross-sections were included: a comparatively stable section used as a spatial baseline, Point I, and Point II. The two eroding points were selected because they displayed visible bank loss and measurable geometric modification. The baseline represents a reference condition at another location rather than a pre-erosion survey of either eroding point. Consequently, all cross-sectional comparisons are spatial and should not be interpreted as direct temporal rates of channel change.

Field equipment described in the source dataset included a measuring tape, measuring rod, GPS or digital mapping support, a camera or smartphone, field notes, and standard data-processing software. Channel width and depth ordinates were recorded at each section. The baseline width was 26.0 m, Point I was 24.0 m, and Point II was 20.0 m. The three interior depth measurements were 0.70, 1.20, and 0.80 m at the baseline; 0.67, 1.00, and 0.78 m at Point I; and 0.70, 1.05, and 0.90 m at Point II. For reconstruction, both bank edges were treated as zero-depth reference points, producing five ordinates for each section. Equal horizontal spacing between adjacent ordinates was applied within each section because no alternative spacing information was available in the dataset.

The analytical workflow was deliberately tiered. First, the raw geometry was checked and reconstructed independently. Second, erosion dimensions were converted into volumes and summarized by bank side. Third, a bounded asymmetry index was derived to describe lateral concentration. Fourth, the two grain-size curves were compared as descriptive material signatures. Finally, the measurements were interpreted as geomorphic evidence of susceptibility rather than as inputs to a factor-of-safety model. Figure 1 summarizes this evidence chain.

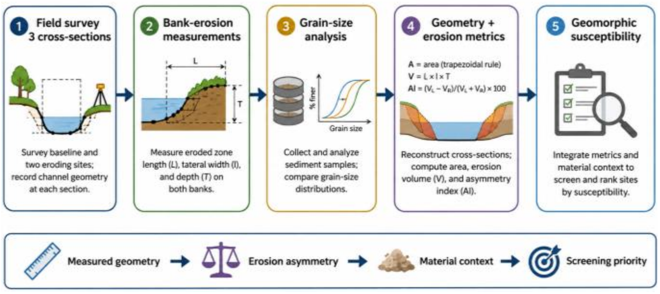

Figure 1. Analytical workflow linking field measurements to geomorphic screening. Source: author's analysis of field data.

2.2 Cross-sectional reconstruction and data quality control

Cross-sectional area was calculated by the trapezoidal rule, $A = \Sigma[(h_i + h_{(i+1)})/2]\Delta x$, where h_i and $h_{(i+1)}$ are adjacent depth ordinates and Δx is the horizontal distance between them. With five ordinates per section, the channel width was divided into four equal intervals. This approach is mathematically transparent and directly reproducible from the recorded field values.

Data-quality control identified an internal inconsistency in the original field-data summary. Summary values of 70.20, 58.80, and 53.00 m^2 were reported for the baseline, Point I, and Point II, respectively, whereas the explicit segment-by-segment trapezoidal calculations for Point I and Point II yielded 14.70 and 13.25 m^2. Recalculation from the recorded widths and depth ordinates showed that each summary value was exactly four times the corresponding trapezoidal area. The internally consistent areas are therefore 17.55 m^2 for the baseline, 14.70 m^2 for Point I, and 13.25 m^2 for Point II. These corrected values are used throughout this manuscript. The correction changes only the geometry comparison; it does not alter the direct field measurements of erosion-zone dimensions or the reported erosion volumes.

2.3 Erosion-volume and asymmetry metrics

Bank erosion was represented by the dimensions of visibly eroded zones. Eroded volume was calculated as $V = P \times L \times T$, where P is the measured length of the eroded zone, L is its lateral width, and T is the mean erosion depth. At Point I, the right-bank dimensions were 2.83 × 2.00 × 1.00 m and the left-bank dimensions were 9.90 × 7.00 × 1.00 m. At Point II, the corresponding right-bank dimensions were 1.98 × 1.40 × 1.00 m and the left-bank dimensions were 5.66 × 4.00 × 1.00 m. The resulting site totals were 74.96 m^3 at Point I and 25.41 m^3 at Point II.

Two additional metrics were derived to make the lateral distribution of erosion explicit. The left-bank share was calculated as $V_L/(V_L + V_R) \times 100$. An erosion asymmetry index (AI) was defined as $AI = (V_L - V_R)/(V_L + V_R)$. AI is bounded from -1 to +1, with positive values indicating left-bank dominance, negative values indicating right-bank dominance, and values near zero indicating comparatively balanced erosion. The index is used only as a descriptor of measured spatial concentration; it is not presented as a calibrated hazard index or a geotechnical stability criterion.

2.4 Grain-size analysis

Two bank-material samples were characterized by sieve analysis. Sample 1 corresponds to Point I and Sample 2 to Point II. Percent-passing values were available for sieve openings of 4.75, 2.35, 1.18, 0.60, 0.45, 0.30, 0.15, and 0.075 mm. Because the available sieve range and ancillary soil data were insufficient for a complete engineering classification, the analysis focuses on direct comparison of the two distribution curves rather than assigning a formal Unified Soil Classification System group.

Similarity between the two curves was summarized descriptively using the Pearson correlation coefficient across the eight common sieve sizes, the mean absolute difference in percent passing, and the root-mean-square difference. These quantities compare curve shape and magnitude only. The sieve points are ordered components of the same distribution and are not independent experimental replicates; therefore, no inferential significance test is attached to the correlation. This distinction is important because material erodibility can also depend on cohesion, density, fabric, chemistry, moisture, and roots, none of which were measured in the source dataset.

2.5 Physical bank-susceptibility framework

The study interprets physical bank susceptibility from converging evidence rather than from a single threshold. The primary evidence is the estimated erosion-zone volume because it provides a direct field-based approximation of the magnitude of visible bank loss. The secondary evidence is lateral asymmetry, which identifies whether loss is concentrated on one bank. Cross-sectional geometry provides contextual evidence about channel form, while grain-size comparison constrains the extent to which differences in particle-size distribution can plausibly explain the site contrast. A site showing larger material loss, strong lateral concentration, and greater geometric disturbance is therefore ranked as more susceptible within the observed dataset.

The terminology is intentionally conservative. Formal bank stability analysis normally requires resisting and driving forces informed by soil strength, unit weight, geometry, groundwater or pore-water conditions, and hydraulic loading. The present study did not measure cohesion, internal friction angle, soil unit weight, pore-water pressure, groundwater variation, or concurrent near-bank velocity. It also did not apply Bishop, Fellenius, Morgenstern-Price, BSTEM, SLOPE/W, PLAXIS, or another process-based geotechnical model. No factor of safety is therefore reported. The outcome is a relative geomorphic screening that identifies priority locations for subsequent investigation.

2.6 Statistical analysis

The field design contains two eroding sites and one comparative baseline, each represented by a single cross-sectional survey. Conventional hypothesis tests, regression models, and confidence intervals would imply replication that the dataset does not provide. The statistical strategy therefore emphasizes descriptive effect metrics with direct physical meaning: absolute and percentage differences in cross-sectional area, site erosion-volume ratio, contribution to combined erosion, left-to-right erosion ratio, bank-side shares, asymmetry indices, and descriptive similarity of grain-size curves. This strategy avoids manufacturing statistical significance from pseudo-replication while extracting the maximum defensible quantitative information from the available measurements.

3. Results and Discussion

3.1 Cross-sectional geometry and data quality

The reconstructed cross-sections show clear spatial differences in channel geometry. The baseline section was 26.0 m wide, had a maximum recorded depth of 1.20 m, and yielded a trapezoidal area of 17.55 m^2. Point I was 24.0 m wide with a maximum depth of 1.00 m and an area of 14.70 m^2. Point II was 20.0 m wide with a maximum depth of 1.05 m and an area of 13.25 m^2. Relative to the baseline, Point I was 7.69% narrower and had a 16.24% smaller reconstructed area, whereas Point II was 23.08% narrower and had a 24.50% smaller area (Table 1).

Table 1. Cross-sectional geometry and descriptive contrasts

Section	Width (m)	Maximum depth (m)	Recomputed area (m^2)	Area vs baseline
Baseline	26.00	1.20	17.55	Reference
Point I	24.00	1.00	14.70	-16.24%
Point II	20.00	1.05	13.25	-24.50%

Note. Areas were recomputed from the recorded five-ordinate cross-sections using a consistent trapezoidal rule.

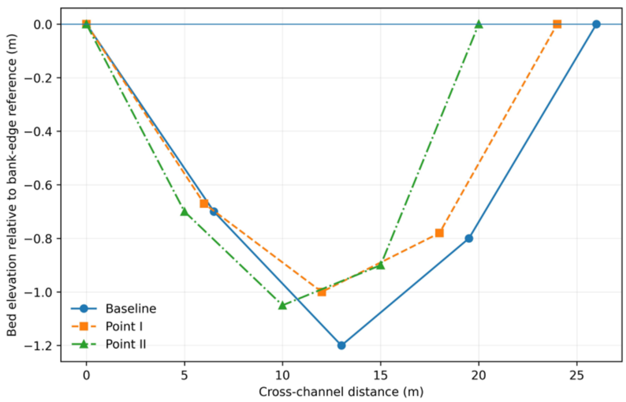

Figure 2. Reconstructed cross-sectional profiles for the baseline, Point I, and Point II. The profiles show spatial differences in channel form; they are not temporal erosion trajectories. Source: author's analysis of field data.

Figure 2 shows that the three profiles are not simply scaled versions of one another. The baseline has the largest reconstructed area and deepest central ordinate, whereas the two eroding sites display different profile shapes and reduced widths. Because the sections were surveyed at different locations and discharge was not standardized, these differences cannot be treated as temporal erosion rates or attributed solely to bank retreat. They instead establish the geometric context within which the direct bank-loss measurements are interpreted.

The second major contribution is methodological: the analysis separates direct evidence of bank loss from supporting evidence of cross-sectional form. The erosion volumes are based on measured dimensions of visible erosion zones and therefore provide the strongest quantitative contrast between Point I and Point II. Cross-sectional areas, by contrast, represent the geometry of three different locations under the field conditions present during survey. The corrected areas of 17.55, 14.70, and 13.25 m^2 show spatial differences in channel form, but they do not quantify how much area was lost through time. This distinction is important because channel geometry can respond to stage, sediment transport, bar configuration, and bed adjustment as well as to lateral bank retreat.

Recent literature illustrates why cross-sectional geometry should be interpreted as part of a coupled morphodynamic system. Xia et al. [24] linked bank retreat volumes to broader channel adjustment in the Jingjiang reach and reported that cross-sectional form changed with the balance between bank retreat and revetment. Vázquez-Vázquez-Tarrío et al. [25] emphasized that sediment transport influences erosion, aggradation, channel geometry, and flood-stage behavior, while Koohizadeh Dehkordi et al. [8] used multitemporal imagery to quantify long-term bank displacement and width change. These studies operate at scales and temporal resolutions beyond the Pattalasang snapshot, but they reinforce a key interpretive rule: cross-sectional differences are not equivalent to erosion rates unless repeat surveys or other temporal evidence establish actual boundary movement.

The arithmetic correction of the source areas is therefore consequential. The original summary values were exactly four times the values produced by the recorded five-ordinate trapezoidal geometry. Using the uncorrected numbers would preserve relative ordering but inflate all section areas and distort any derived interpretation of channel capacity. In a small dataset, transparent verification of deterministic calculations may have greater analytical value than adding a more complicated statistical test. This is especially relevant for rapid field assessments, where decision usefulness depends on traceability from raw measurements to derived indicators. Goode et al. [20] similarly emphasize the value of direct geomorphic observation for detecting instability, while Kassa et al. [19] show that analytical sophistication does not compensate for a mismatch between model structure and the processes represented by the available data.

The erosion-volume contrast is physically meaningful even though the volume approximation is simple. Point I had 2.95 times the measured loss of Point II. Experimental and modelling studies commonly separate lower-bank hydraulic removal from subsequent mass failure. Wang et al. [26] describe a two-stage sequence of toe cutting followed by bank collapse, and Bigham et al. [4] found toe erosion to be the dominant streambank process under both regulated and unregulated scenarios in their study. This process logic supports the interpretation that greater toe-area material loss can progressively alter support conditions for the upper bank. It does not, however, establish a factor of safety or prove imminent failure at Pattalasang.

3.2 Bank-erosion magnitude and lateral asymmetry

Measured erosion differed substantially between the two eroding sites. Point I contained 74.96 m^3 of eroded material, compared with 25.41 m^3 at Point II. The site-volume ratio was therefore 2.95, and the absolute difference was 49.55 m^3. Of the combined 100.37 m^3 measured at the two sites, Point I contributed 74.68% and Point II 25.32%. The magnitude of this contrast provides the clearest basis for ranking Point I as the more severely affected site.

The bank-side distribution was even more strongly differentiated (Table 2; Figure 3). At Point I, left-bank erosion was 69.30 m³ and right-bank erosion was 5.66 m³, a left-to-right ratio of 12.24:1. The left bank accounted for 92.45% of the site total, producing an AI of 0.849. At Point II, left-bank erosion was 22.64 m³ and right-bank erosion was 2.77 m³, a ratio of 8.17:1. The left-bank share was 89.10% and AI was 0.782. Pooled across both sites, 91.60% of the measured loss occurred on the left bank and the combined AI was 0.832. The repeated directional bias is therefore not a minor secondary feature: it is the dominant spatial pattern in the erosion measurements.

Table 2. Erosion magnitude, bank-side contribution, and asymmetry indicators.

Site	Left volume (m³)	Right volume (m³)	Total (m³)	Left Share	Asymmetry index
Point I	69.30	5.66	74.96	92.45%	0.849
Point II	22.64	2.77	25.41	89.10%	0.782
Combined	91.94	8.43	100.37	91.60%	0.832

Note. AI = (Vleft - Vright)/(Vleft + Vright); positive values indicate left-bank dominance.

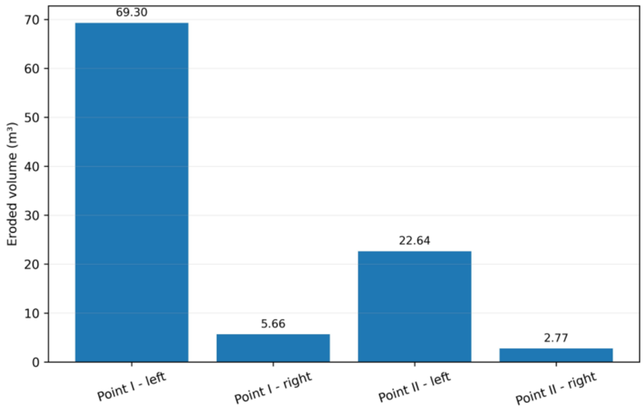

Figure 3. Measured erosion volume by site and bank side. The figure highlights the strong concentration of material loss on the left bank at both eroding sites. Source: author's analysis of field data

The most distinctive empirical result is the consistency of left-bank dominance at both eroding sites. More than 89% of the measured erosion occurred on the left bank at each point, with AI values of 0.849 and 0.782. The repetition of the same directional bias suggests that the measured erosion is organized by local channel processes rather than randomly distributed between banks. Comparable asymmetry has been reported in multitemporal river studies, although the dominant bank varies by system. Akter et al. [1] found erosion-dominant behavior on the left bank of the Kirtankhola River, whereas other basin-scale work documents different left-right balances depending on reach geometry and hydrologic history. Dehkordi et al. [8] specifically reported flood-related asymmetric bank erosion in the Bazoft River, reinforcing the broader point that major events can reorganize erosion spatially rather than uniformly.

The likely mechanism is hydraulic concentration, but the Pattalasang data do not directly measure it. Studies using ADCP observations show that locally elevated boundary shear and altered flow structure can coincide with widening and bank erosion [2]. In the Amazon near Iquitos, streambank erosion was concentrated on the outer concave side of the main channel and intensified during a severe flood [6]. At the Middle Yangtze, near-bank hydraulic erosion remained a primary factor affecting protected-bank erosion even where revetment altered channel adjustment [5]. Laboratory evidence from Makassar also shows that higher discharge increases local scour and that porous deflectors can reduce flow velocity and scour depth around hydraulic structures [9,10]. These studies make preferential hydraulic attack a credible working hypothesis for the Pattalasang left-bank signal, while the difference in setting requires that the mechanism be verified in the field.

Directional asymmetry should not be translated directly into causation. Without measurements of planform curvature, flow vectors, water-surface slope, discharge, or near-bank velocity, the dataset cannot distinguish among curvature-driven secondary circulation, local constriction, roughness contrasts, obstructions, bar-induced steering, or bank-material differences. The literature shows that multiple geometric controls can alter bank exposure. Inoue et al. [15], for example, related flood-era bank erosion to the ratio of bar height to bank height, while Akter et al. [1] associated pronounced instability with highly sinuous river sections. Thus, the asymmetry index is best treated as a diagnostic flag: it identifies where the process is spatially concentrated and defines the hydraulic hypothesis that future measurements must test.

The combined evidence can be organized into a testable mechanistic sequence. Stage 1 is hydraulic exposure, in which local flow structure concentrates stress against a bank. Stage 2 is toe removal, where lower-bank material is detached and transported. Stage 3 is geometric adjustment, where undercutting or steepening reduces support for the upper bank and may permit raveling, slumping, or collapse. Stage 4 is morphodynamic feedback, because the changed bank and cross-section redistribute subsequent flow and sediment transport. Experimental work on bank retreat identifies toe cutting followed by collapse as a coupled sequence [26], while studies of regulated channels and protected banks similarly show the importance of toe erosion and near-bank hydraulic forcing [4,5]. The Pattalasang data directly observe material loss and geometry but not the initiating hydraulic stress or subsequent failure mechanics, so Stages 1 and 3 remain hypotheses to be tested.

3.3 Grain-size characteristics and material controls

The two grain-size distributions were broadly similar in overall form but differed at several intermediate sieve sizes. At 4.75 mm, 55.35% of Sample 1 and 52.30% of Sample 2 passed. At 0.075 mm, the passing fractions were 3.95% and 3.00%, respectively. The largest differences occurred at 2.35, 1.18, and 0.60 mm, where Sample 1 generally showed a higher passing percentage.

Across the eight common sieve openings, the descriptive Pearson correlation between the curves was r = 0.941. The mean absolute difference was 6.58 percentage points and the root-mean-square difference was 8.77 percentage points. Figure 4 therefore shows two curves with a strong common pattern rather than two fundamentally different gradations.

Because Point I nevertheless experienced 2.95 times the total erosion volume of Point II, particle-size distribution alone is not sufficient to explain the observed site contrast. This conclusion is restricted to the measured grain-size data and does not exclude differences in cohesion, soil fabric, density, moisture, chemistry, or vegetation.

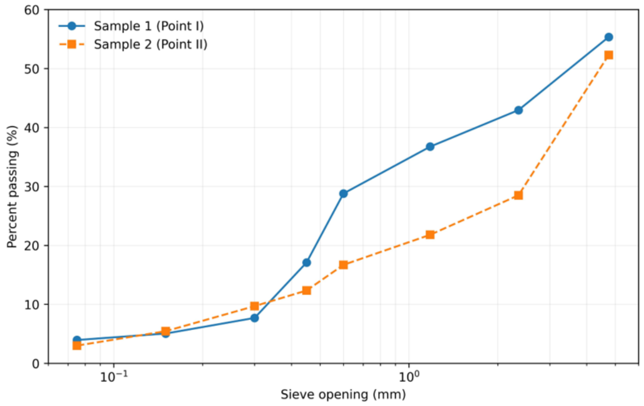

Figure 4. Grain-size distribution curves for bank-material samples from Point I and Point II. Their broadly similar shapes constrain, but do not eliminate, material-property explanations for the erosion contrast. Source: author's analysis of field data.

The grain-size comparison constrains but does not resolve the material-control question. The two distributions are highly concordant in shape, with r = 0.941 across the common sieve openings, while the erosion-volume contrast approaches threefold. If particle-size distribution were the dominant control and all other conditions were comparable, a much stronger material contrast might be expected. The available evidence therefore argues against a single-variable explanation based on gradation alone. This inference is consistent with recent work showing that bank resistance can vary substantially within nominally similar sediments because erodibility depends on properties not captured by sieve curves.

Wilson et al. [27] found spatial differences in critical shear stress associated with soil texture and bulk density, illustrating that mechanical resistance cannot be inferred from particle-size distribution alone. Li et al. [16] further showed that bank migration in an unvegetated meandering river was related to sedimentological, geochemical, and microbial differences, with cavity-rich and compact layers behaving differently. At the process scale, Smith et al. [17] demonstrated strong reductions in fluvial erosion when root reinforcement and organic-mediated extracellular products were present, while Zong et al. [18] reported that vegetation roots increased critical shear stress and reduced soil erodibility in field experiments. The Pattalasang dataset contains none of these complementary measurements, so the similar sieve curves should be interpreted as evidence of incomplete material differentiation rather than as evidence that the two banks have identical resistance.

Vegetation is particularly important because its effects can be both mechanical and hydraulic. Biggs et al. [28] found greater geomorphic change where riparian vegetation was removed during extreme flooding, whereas the systematic review by Hardwick et al. [29] noted that the vegetation-bank erosion literature still contains limited quantitative geomorphic evidence and strong context dependence. Controlled experiments by Li et al. [30] showed that both root mass density and vegetation discontinuity influence erosion and near-bank flow structures. These findings support two implications for Pattalasang. First, unmeasured vegetation differences could contribute to the Point I-Point II contrast. Second, future surveys should quantify vegetation cover and root-zone condition rather than record vegetation qualitatively.

The same caution applies to soil-water interactions. Integrated riverbank investigations show that hydraulic forcing, bank geometry, soil strength, and saturation conditions jointly affect failure potential [11,13,14]. The Pattalasang study should therefore not infer geotechnical stability from grain size or erosion volume alone. Its contribution lies in showing where the observable evidence is strongest and which missing measurements are required to move from geomorphic susceptibility to formal stability analysis.

3.4 Integrated susceptibility, monitoring, and management

Integration of the field metrics produces a consistent relative ranking. Point I combines the largest total erosion volume, the strongest left-bank concentration, and marked local geometric disturbance. Point II shows the same directional asymmetry but at lower erosion magnitude. The baseline has no comparable measured erosion volume in the dataset and functions as a geometric reference. Point I is therefore designated the highest-priority location for follow-up hydraulic and geotechnical assessment, Point II a secondary priority, and the baseline a monitoring reference. These categories are relative screening outcomes and should not be interpreted as engineering safety classifications.

The results support a three-tiered assessment framework. Tier 1 is the low-cost geomorphic screen demonstrated here: fixed cross-sectional geometry, measured erosion dimensions, bank-side attribution, standardized photographs, and basic material screening. The outputs are transparent effect metrics rather than model-dependent probabilities. Tier 2 adds repeat surveys, water level, discharge or velocity, planform geometry, vegetation mapping, and more detailed sediment characterization. Tier 3 adds geotechnical strength testing, groundwater monitoring, and process-based stability modelling. This sequence reflects the literature rather than opposing simple and advanced methods. Integrated studies achieve stronger causal diagnosis precisely because they combine morphology, hydrology, and material properties [1,11-13].

The value of Tier 1 is prioritization. Manopkawee [23] used integrated fluvial-landscape parameters to identify erosion hotspots and susceptible reaches, demonstrating the management value of screening before intervention. Rapid geomorphic assessment can likewise reveal process trajectories that point measurements miss [20]. In Pattalasang, the 74.96 m³ erosion volume and AI of 0.849 at Point I provide a clear basis for allocating the next round of monitoring there first. Point II should be retained as a comparison site because it shares the same left-bank bias but at lower magnitude. The baseline should remain a reference section, preferably resurveyed under comparable flow conditions.

Intervention should follow process diagnosis. Field and experimental studies show that vegetation can increase erosion resistance through root reinforcement, although its effectiveness depends on the continuity of cover and the surrounding flow field [17,18,28,30]. Where severe toe scour is the dominant process, a surface-only treatment may leave the hydraulic driver unchanged. Hydraulic countermeasures can redirect or dissipate local flow energy, as shown by groyne modelling in the Padma River [31] and by recent porous-deflector experiments that reduced local velocity and scour [9,10]. These studies do not provide a design for Pattalasang; they indicate that any intervention should be selected only after the dominant failure mechanism, design flow, toe-scour depth, foundation condition, and potential transfer of erosion are established.

The management implication is equally conditional. Point I is the first priority for information gain because it combines the largest measured volume loss with the strongest asymmetry. If monitoring confirms active toe scour, protection should address the lower bank and the flow field before relying on surface stabilization. Hydraulic modelling of groyne configurations shows that appropriately designed structures can redirect high-velocity flow and reduce near-bank shear and scour, although such interventions require reach-specific calibration [31]. Conversely, experiments with emergent vegetation show that vegetation can reduce bank erosion but can also alter local turbulence and channel erosion patterns, especially where sediment mining or discontinuous cover changes the flow field [32]. This reinforces the principle that erosion-control measures should be matched to the identified mechanism rather than selected solely because they are conventional.

Catchment and reach context should also be considered before local works are designed. Watershed-scale erosion can alter sediment delivery and downstream channel conditions [33], while regional erosion-hazard mapping in Sulawesi shows the importance of slope, erodibility, land cover, and conservation priorities [34]. At the reach scale, sediment supply and transport influence the morphology against which local bank protection operates [25]. A rigid protection measure that halts retreat at one bank can redistribute shear, alter bed incision, or move erosive energy downstream; Zhou et al. [5] reported such trade-offs for protected banks in the Middle Yangtze. Thus, a local intervention at Pattalasang should be evaluated as part of a channel system rather than as an isolated slope.

The proposed diagnostic is therefore best viewed as the first step of adaptive management. It identifies the most severely affected site, specifies the dominant spatial pattern, clarifies which measurements are missing, and provides a baseline against which future change can be evaluated. If subsequent monitoring verifies persistent left-bank hydraulic concentration and continued toe loss, the case for targeted intervention will be substantially stronger. If instead the asymmetry weakens or shifts, the dataset will indicate that erosion is episodic or controlled by changing local conditions. Either outcome improves decision quality because the management response becomes tied to observed process evolution rather than a single reconnaissance visit.

3.5 Limitations, future research, and scientific contribution

The limitations are substantial and define the boundary of the claims. First, the design contains only two eroding points and one baseline section, so it cannot estimate reach-wide probability, temporal erosion rate, or statistical population parameters. Second, the sections are spatially distinct and were not surveyed repeatedly under standardized stage conditions. Third, hydraulic forcing was not measured concurrently, leaving the proposed explanation for left-bank dominance inferential. Fourth, only two bank-material samples were available, and cohesion, density, moisture, plasticity, chemistry, root density, and groundwater conditions were not measured. Fifth, the erosion-volume method estimated volume of the measured erosion zone. Sixth, the baseline is a comparator rather than a reconstructed pre-erosion condition for either eroding site.

These limitations are not unusual in reconnaissance datasets, but they prevent several stronger claims. The study cannot state that Point I is geotechnically unstable, because factor of safety was not calculated. It cannot state that the 16.24% and 24.50% differences in cross-sectional area were caused by erosion through time, because repeat surveys are absent. It cannot attribute the left-bank pattern uniquely to bend hydraulics, because velocity and curvature data are unavailable. It also cannot conclude that grain size is unimportant; the evidence only shows that the measured gradation difference is insufficient by itself to account for the observed erosion-volume contrast.

Future research should therefore convert the current spatial snapshot into an event-based monitoring design. The most efficient program would establish permanent cross-section monuments and bank pins, resurvey after hydrologically significant events, record water level and discharge or near-bank velocity, measure local bank angle and toe position, and map vegetation cover. Photogrammetry or lidar could then provide independent volumetric validation. Similar repeated approaches have shown that bank retreat can be highly episodic and strongly site dependent [35], while flood-focused geomorphic studies demonstrate that extreme events can generate localized responses that differ from long-term average behavior [7].

The geotechnical upgrade should include water content, bulk density, gradation, Atterberg limits where appropriate, cohesion, friction angle, and groundwater or pore-water information. Formal stability modelling could then test whether the geomorphic ranking corresponds to calculated safety margins. Recent hydro-geotechnical river studies demonstrate how field hydraulics and material properties can be combined to diagnose river-induced instability [11,13], while Indonesian riverbank stability work illustrates the value of formal slope analysis once the required parameters are available [14].

The scientific contribution of the present study is therefore methodological rather than universal. It demonstrates a disciplined way to extract decision-relevant information from a limited dataset without disguising missing process measurements. The novelty lies in the combination of four elements: explicit arithmetic quality control, direct erosion-volume comparison, a transparent left-right asymmetry metric, and material-curve comparison interpreted within a clearly bounded susceptibility framework. In the supplied literature, many studies operate either at broad spatial scales using remote sensing or at detailed process scales using hydraulic and geotechnical models. The Pattalasang workflow occupies the intermediate reconnaissance space and provides a traceable bridge from low-cost field evidence to the design of the next, more mechanistic investigation.

4. Conclusion

This study developed a field-based geomorphic diagnostic for erosion-related bank susceptibility in the Pattalasang River using only measurements supported by the available dataset. Recalculation of the five-ordinate cross-sections resolved a factor-of-four inconsistency in the source summary and produced internally consistent areas of 17.55 m² for the baseline, 14.70 m² for Point I, and 13.25 m² for Point II. The correction demonstrates that arithmetic quality control is essential before morphological comparisons are interpreted.

The principal empirical finding is the magnitude and directionality of bank erosion. Point I contained 74.96 m³ of measured eroded material, 2.95 times the 25.41 m³ measured at Point II. Left-bank erosion contributed 92.45% and 89.10% of the site totals, producing asymmetry indices of 0.849 and 0.782. This repeated left-bank bias is the strongest field signal in the dataset and establishes a testable hypothesis of bank-specific hydraulic concentration.

The two grain-size distributions were broadly concordant, so the large contrast in erosion volume cannot be explained by measured gradation alone. Literature-based comparison indicates that bank response is more plausibly governed by interactions among hydraulics, geometry, soil structure and strength, moisture or seepage, and vegetation. Because these variables were not fully measured, the results are intentionally expressed as relative geomorphic susceptibility rather than factor-of-safety-based stability.

Point I should therefore receive the highest priority for repeat cross-sectional monitoring, bank-retreat measurement, hydraulic observation, and geotechnical sampling, with Point II retained as a lower-magnitude comparison site. The broader contribution is a tiered assessment logic in which transparent, low-cost field metrics identify where detailed hydraulic and geotechnical analysis will provide the greatest value. This preserves analytical rigor while making limited field datasets useful for practical riverbank management.

The practical value of this method lies in converting limited but auditable measurements into testable monitoring priorities without overstating geotechnical certainty.

Declaration of generative AI and AI-assisted technologies in the manuscript preparation process

During the preparation of this work, OpenAI ChatGPT was used to support manuscript organization, language refinement, and the presentation of calculations derived from the study data. All authors subsequently reviewed and edited the manuscript and independently verified the data, calculations, references, interpretations, and scientific conclusions. The authors take full responsibility for the accuracy, integrity, and content of the published work.

CRediT authorship contribution statement

Sri Winanda: Conceptualization, Methodology, Investigation, Data curation, Formal analysis, Visualization, Writing – original draft, Writing – review & editing. **Marufah**: Investigation, Data curation, Validation, Resources, Writing – review & editing. **Muh Yunus Ali**: Methodology, Validation, Supervision, Project administration, Writing – review & editing.

Funding

This research received no specific grant from funding agencies in the public, commercial, or not-for-profit sectors.

Declaration of competing interest

The authors declare that they have no known competing financial interests or personal relationships that could have appeared to influence the work reported in this paper.

Data availability

All numerical data supporting the findings of this study are presented within the manuscript, tables, and figures. Additional information related to the field measurements may be made available by the corresponding author upon reasonable request.

References

[1] Akter R, Mahmud MI, Mia AJ, Ahmed F, Alam MF, Farazi AH, et al. Integrated geospatial, geotechnical, and hydrologic analysis of bank dynamics in the Kirtankhola River, Bangladesh. International Journal of River Basin Management. 2026.

[2] Bhattacharya RK, Das Chatterjee N, Das K. Channel instability and hydrogeomorphic adjustment in alluvial reach of Kangsabati River, India using Digital Shoreline Analysis System and Acoustic Doppler Current Profiler. Geocarto International. 2022;37(27):16232-60.

[3] Koohizadeh Dehkordi A, Fatahi Nafchi R, Samadi-Boroujeni H, Khastar Boroujeni M, Ostad–Ali–Askari K. Assessment of morphological changes of river bank erosion using landsat satellite time-series images. Ain Shams Engineering Journal. 2024;15(3).

[4] Bigham KA, Keane TD, Moore TL. Effect of flow regulation on streambank erosion: A perspective downstream of a flood control dam, Kansas, USA. River Research and Applications. 2024;40(1):14-28.

[5] Zhou Y, Xia J, Deng S, Han Z. Bank erosion under the impacts of hydraulic erosion, river stage change and revetment protection in the Middle Yangtze River. Geomorphology. 2024;448.

[6] Angulo KG, Lee KT. Detecting the Planform Changes Due to the Seasonal Flow Fluctuation and 2012 Severe Flood in the Amazon River near Iquitos City, Peru Based on Remote Sensing Image Analysis. Water (Switzerland). 2022;14(3).

[7] Dawson M, Lewin J. The heterogeneous geomorphological impact of an exceptional flood event and the role of floodplain vegetation. Earth Surface Processes and Landforms. 2024;49(1):354-73.

[8] Dehkordi AK, Khastar Boroujeni M, Nikoo MR, Sadra N, Nafchi RF, Boroujeni HS. Unveiling hidden dynamics of river morphology:

Insights from the 2010 flash flood and Karun-4 dam impact in Southwestern Iran. Journal of Hydrology. 2025;661.
[9] Baharuddin A, Karim N, Ali MY, Latif S. Investigasi eksperimental pengendalian gerusan pilar jembatan menggunakan deflektor arus bawah air berpori. Journal of Green Complex Engineering. 2026;3(2):83-94.
[10] Nurizkitha IZ, Karim N, Al Imran H, Latif S. Efektivitas deflektor silinder pori bertulang dalam mengurangi kecepatan aliran di sekitar pilar jembatan. Journal of Green Complex Engineering. 2026;3(2):73-82.
[11] Andriani A, Istijono B, Hakam A, Mahdi M, Yuhendra R, Dodi A, et al. Hydro-geotechnical integration for sustainable mitigation of river-induced landslides along the Batang Ombilin River, West Sumatra. Geoenvironmental Disasters. 2026;13(1).
[12] Okeke CAU, Uno J, Academe S, Emenike PGC, Abam TKS, Omole DO. An integrated assessment of land use impact, riparian vegetation and lithologic variation on streambank stability in a peri-urban watershed (Nigeria). Scientific Reports. 2022;12(1).
[13] Rojas AF, Rojas LEA, Gonzalez EAP, Ortiz STF, Alonso JCA. Geomorphological and geotechnical conditions that determine susceptibility to bank erosion and meander migration in the Unete River channel affecting the road infrastructure. Investigaciones Geograficas. 2024.
[14] Yusuf K, Al Hadi Y, Maulani E, Akbar SJ, Arfiandi J. Analisis stabilitas lereng Sungai Tamiang Kampung Rantau Pakam. Teras Jurnal: Jurnal Teknik Sipil. 2023;13(2):469-80.
[15] Inoue T, Hiramatsu Y, Johnson JPL, Dempo J, Mishra J. Ratio of River Channel Bar to Bank Height Sets Bank Erosion Rate. Journal of Geophysical Research: Earth Surface. 2025;130(1).
[16] Li J, Grenfell MC, Cheng D, Alhassan J. Biogeochemical controls on soil dispersion and bank stability in the unvegetated, meandering Sulengguole River, Qaidam Basin, China. Progress in Physical Geography. 2025;49(5):615-34.
[17] Smith DJ, Wynn-Thompson TM, Stremler MA, Williams MA, Seiler JR, Hession WC. Root reinforcement and extracellular products reduce streambank fluvial erosion. Science of the Total Environment. 2023;896.
[18] Zong Q, Zhang Y, Tang R, Tang H, Liu H, Li L. Field experiment on the influence of vegetation roots on riverbank erosion characteristics in the Tarim River. Shuikexue Jinzhan/Advances in Water Science. 2024;35(2):232-43.
[19] Kassa K, Castro-Bolinaga C, Guertault L, Fox GA, Russell P, Brown ED. Quantifying the Impact of Model Selection When Examining Bank Retreat and Sediment Transport in Stream Restoration. Water (Switzerland). 2023;15(8).
[20] Goode JR, Hawley RJ, Lewis RH, Mulhall B. Rapid geomorphic assessment walkabouts as a tool for stream mitigation monitoring. Journal of the American Water Resources Association. 2024;60(5):991-1007.
[21] Lo HW, van Leeuwen Z, Klaar M, Woulds C, Smith M. Geomorphic effects of natural flood management woody dams in upland streams. River Research and Applications. 2022;38(10):1787-802.
[22] Faisal BMR, Hayakawa YS. Geomorphological processes and their connectivity in hillslope, fluvial, and coastal areas in Bangladesh: A review. Progress in Earth and Planetary Science. 2022;9(1).
[23] Manopkawee P. Identifying erosional hotspots in the Mae Chan River watershed, northern Thailand using integrated fluvial landscape dynamic parameters. Natural Hazards. 2025;121(19):23379-416.
[24] Xia J, Liu X, Deng S, Zhou M, Li Z, Peng Y. Temporal and spatial distribution of bank retreat in the Jingjiang reach of the Yangtze River after the Three Gorges Project operation and its influence on channel adjustment. Hupo Kexue/Journal of Lake Sciences. 2022;34(1):296-306.
[25] Vázquez-Tarrío D, Ruiz-Villanueva V, Garrote J, Benito G, Calle M, Lucía A, Díez-Herrero A. Effects of sediment transport on flood hazards: Lessons learned and remaining challenges. Geomorphology. 2024;446.
[26] Wang X, Chen J, Chen X, Chen H, Zhao W, Ruan H, Wang J. Bank Retreat Mechanisms Driven by Debris Flow Surges: A Parameterized Model Based on the Results of Physical Experiments. Water Resources Research. 2024;60(7).
[27] Wilson CG, Schilling KE, Thanos Papanicolaou AN. EVALUATING CAUSAL FACTORS THAT INFLUENCE THE SPATIAL AND TEMPORAL VARIABILITY OF STREAMBANK EROSION IN IOWA. Journal of the ASABE. 2022;65(6):1465-73.
[28] Biggs H, Haddadchi A, Brasington J, Bind J, Stout J. The impact of riparian vegetation on bank erosion during extreme weather events. Earth Surface Processes and Landforms. 2025;50(10).
[29] Hardwick J, Hackney C, Keen L, Fitzsimmons C, Willby N, Pattison Z. The Role of Non-Native Plant Species in Modulating Riverbank Erosion: A Systematic Review. River Research and Applications. 2025;41(4):757-72.
[30] Li JF, Chiang YC, Chen SC. Experimental investigation of root mass density and vegetation discontinuity effects on riverbank erosion. Journal of Hydrology. 2026.
[31] Shahariar S, Sultana N, Zobeyer H. Groynes in riverbank erosion control: An integrated hydrodynamic and morphodynamic modelling for a selected reach of the Padma river. Environmental Earth Sciences. 2025;84(16).
[32] Arora S, Kumar B. Effect of emergent vegetation on riverbank erosion with sediment mining. Scientific Reports. 2024;14(1).
[33] Chalid A, Suhirna U, Siregar CA. Analisis pengaruh erosi lahan pada Daerah Aliran Sungai Ciujung Kabupaten Lebak. Jurnal Talenta Sipil. 2022;5(1):144.
[34] Takwim S, Basri IS, Ramadhan A. Integrasi USLE-SIG dan zonasi konservasi untuk mitigasi bencana: Studi kasus Desa Poi, Sigi. Jurnal LINEARS. 2025;8(2):157-72.
[35] Leroy JZ, Heimann DC, Hix KD, Cigrand CV, Burk TJ. Geomorphic Change, Hydrology, and Hydraulics of Caulks Creek, Wildwood, Missouri. 2024.

This page is intentionally left blank.

Journal of Green Complex Engineering